NONDESTRUCTIVE/IN-FIELD CHARACTERIZATION OF TENSILE PROPERTIES AND RESIDUAL STRESS OF WELDED STRUCTURES USING ADVANCED INDENTATION TECHNIQUE

by Yeol Choi[1]*, Dongil Son[1], Kwang-Ho Kim[1], S. Joon Park[1], Jae-il Jang[1] and Dongil Kwon[2]

[1]Frontics, Inc., Research Institute of Advanced materials, Seoul National University,
Seoul 151-742, Korea, ychoi@frontics.com
[2]School of Materials Science and Engineering, Seoul National University,
Seoul 151-742, Korea, dongilk@gong.snu.ac.kr

ABSTRACT

Structural integrity assessment is indispensable for preventing catastrophic failure of industrial structures/components/facilities. This diagnosis of operating components should be done periodically for safe maintenance and economical repair. However, conventional standard methods for mechanical properties have the problems of bulky specimen, destructive and complex procedure of specimen sampling. Especially, the mechanical properties at welded zone including weldment and heat affected zone could not be evaluated individually due to their size requirement problem. So, an advanced indentation technique has been developed as a potential method for non-destructive testing of in-field structures. This technique measures indentation load-depth curve during indentation and analyzes the mechanical properties related to deformation such as yield strength, tensile strength and work-hardening index. Also indentation technique can evaluate a residual stress based on the concept that indentation load-depth curves were shifted with the direction and the magnitude of residual stress applied to materials. In this study, we characterized the tensile properties and welding residual stress of various industrial facilities through the new techniques, and the results are introduced and discussed.

KEYWORDS
Advanced indentation technique, tensile properties, welding residual stress, non-destructive test

1. INTRODUCTION

Recently, the reliability diagnosis of the in-service materials takes interest with frequent failure of structural components by a time-dependent degradation and a severe operating environment. Especially, the operating conditions of the pipeline are more severe by the cryogenic contents and many inhomogeneous welded joints. And, the welded joint has been the initiation point of fracture by the effect of the microstructural and mechanical inhomogeneities [1]. Also residual stress occurred by welding is one of the most important factors for the reliability diagnosis. Especially, tensilely stressed region is harmful due to the susceptibility of fatigue and stress corrosion cracking [2].

But, conventional standard tests such as the uniaxial tensile and the fracture mechanics tests, which need the bulky standard samples, cannot be applied to the testing of in-service structure/facilities and local region such as welded joint. Also conventional measurement techniques for residual stress such as hole-drilling, saw-cutting techniques, X-ray, magnetic Barkhausen noise and ultrasonic methods have limitation in application due to their destructive characteristics or the difficult problem of separating the microstructural effects from the effects of residual stress on physical parameters. So, they often show the poor reproducibility and large scatter of testing results in comparing with the mechanical methods. With similar viewpoint, it is almost impossible to use the non-destructive methods for assessment of residual stresses in weldment including heat-affected zones (HAZs), which have very rapid gradient of microstructures. So new mechanical testing method for residual stress evaluation is needed.

To overcome the limitations of both destructive/mechanical and non-destructive / physical methods, a new nondestructive / mechanical indentation technique was developed and used for the quantitative evaluation of tensile properties and residual stresses in weldment in this study.

The advanced indentation technique is developed from the conventional hardness test. This technique provides indentation load-depth curve through measuring the indentation load and penetration depth continuously during loading and unloading by spherical indenter at constant speed, instead of the direct observation and measurement of indent size in the conventional hardness test. The equivalent true stress and strain identical with the flow properties from the standard uniaxial tensile test can be predicted from the analysis of indentation load-depth curve considering the indentation stress fields and deformation shape [3,4].

In this study, we evaluated the flow properties including the yield strength, work-hardening exponent and ultimate tensile strength of girth weld joint of API X65 pipeline steel and the residual stresses of A335 P12 pipeline using advanced indentation technique.

2. THEORY OF ADVANCED INDENTATION

Derivation of tensile properties by advanced indentation technique

As the spherical indenter penetrates into material, mechanical deformation is divided as three stages of elastic, elastic/plastic, fully plastic [5]. The contact mean pressure slightly increases in this fully plastic region. These deformation stages are similar to the work-hardening behavior of the uniaxial tensile test except for non-homogeneity. Researches for predicting the uniaxial flow properties from indentation-induced deformation were done as below. The raw data from the advanced indentation test is the indentation load-depth curve as shown in Fig. 1.

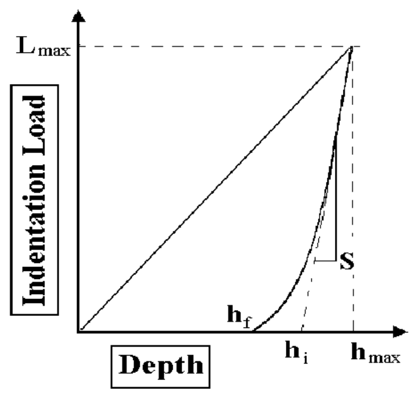

Fig. 1. Schematic graph of the indentation load-depth curve.

The equivalent stress and strain were defined in terms of the measured indentation contact parameters such as contact depth, h_c^*, indenter shape and the morphology of the deformed sample surface. And, real contact properties were determined by considering both the elastic deflection and the material pile-up around the contacting indenter.

Firstly, a contact depth at maximum indentation load can be evaluated by analyzing the unloading curve with the concept of indenter geometry and elastic deflection as shown in Eq. (1) [6].

$$h_c^* = h_{max} - \omega(h_{max} - h_i) \tag{1}$$

h_i is the intercept indentation depth as shown in Fig. 1 and indenter shape parameter, ω is 0.75 for the spherical indenter. Secondly, the material pile-up around indentation enlarges the contact radius from the analysis of elastic deflection. The real contact area is expressed extent as Eq. (2) in terms the geometrical relationship of indenter radius, R and h_c^*, considering this pile-up effect by the work-hardening exponent, n [7,8].

$$a^2 = \frac{5(2-n)}{2(4+n)}(2Rh_c^* - h_c^{*2}) \tag{2}$$

a is the real contact radius considering the pile-up around indent.
So the contact mean pressure, P_m is expressed as Eq. (3).

$$P_m = \frac{L_{max}}{\pi a^2} \tag{3}$$

An equivalent strain, ε_R of indentation is evaluated from the material displacement beneath the indenter along the indentation axis direction as like Eq. (4) [3,4].

$$\varepsilon_R = \frac{\alpha}{\sqrt{1-(a/R)^2}}\frac{a}{R} \quad (4)$$

The equivalent stress, σ_R can be evaluated using the relationship with contact mean pressure as shown Eq. (5) [3,4].

$$\frac{P_m}{\sigma_R} = \Psi \quad (5)$$

Ψ is a constraint factor for plastic deformation and the upper limit is about 3 for fully plastic deformation of steels. The exact values of work-hardening exponent, equivalent stress and strain are calculated by iteration method [3,4]. From the analysis of each unloading curve, both equivalent stress and strain values are determined. The stress and strain relation is fitted as the power-type Hollomon equation expressing work-hardening behavior. The fitted curve was extrapolated to initial yield and ultimate tensile regions. Then, yield strength was evaluated by inputting yield strain to Hollomon equation. And, ultimate tensile strength was evaluated using the concept that uniform elongation is equal to work-hardening exponent.

Evaluation of residual stress using advanced indentation technique

Indentation hardness was used as a parameter of the residual stress in initial studies [9]. However, the variations in the apparent hardness with a change in the residual stress have been identified as an artifact of erroneous optical measurements of the indentation mark. Recently, the intrinsic hardness has been reported as constant regardless of the residual stress in studies using fine observations of the indentation mark [10,11] by scanning electron or atomic force microscopes. Therefore, the change in contact morphologies with residual stress was modeled for constant maximum indentation depth assuming the independence of the intrinsic hardness and the residual stress [12].

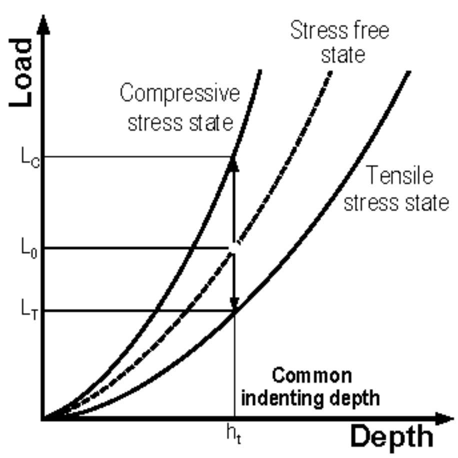

Fig. 2. Variation of the indentation loading curves with the changes in the stress states [13-15].

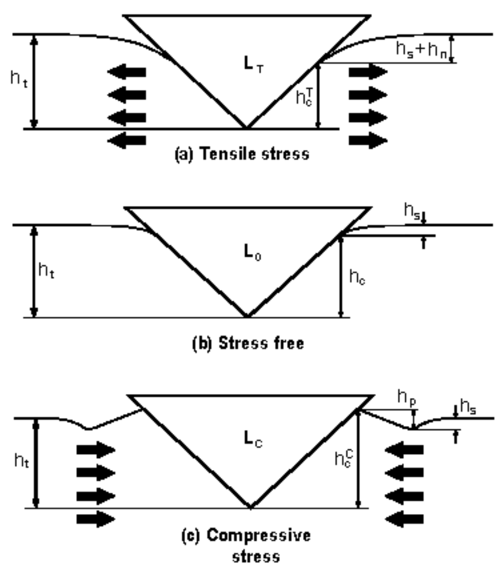

Fig. 3. Theoretical surface morphologies around the contact for (a) tensile stress, (b) stress-free and (c) compressive stress states.

The change in indentation deformation caused by the residual stress was identified in the indentation loading curve shown in Figs. 2. The applied load of the tensile stressed state is lower than that of a stress-free state for the same maximum indentation depth [10-12]. In other words, the maximum indentation depth desired is reached at a smaller indentation load in a tensile stressed film, because a residual-stress-induced normal load acts as an additive load to the applied load. Therefore, the residual stress can be evaluated by analyzing the residual-stress-induced normal load.

The detailed changes in contact morphology can be explained from the schematic diagram shown in Fig. 3 (a) and (b). The residual stress is relaxed for a tensile stressed specimen maintaining the constant maximum depth, h_t, as the stress relaxation pushes the indenter out from the surface. However, the pushing force appears as increases in the applied load ($L_T \rightarrow L_0$) and the contact depth ($h_c^T \rightarrow h_c$), because the maximum depth is held constant. The indentation load and maximum depth for the tensile stressed state (L_T, h_t) is equivalent to those in the relaxed state (L_0, h_t). Thus, the relationship between the two states can be expressed as

$$L_0 = L_T + L_{res} \tag{6}$$

In the compressive stress state, the applied load and contact depth decrease by stress relaxation under the maximum-depth-controlled path. Furthermore, this decreasing portion of the applied load was the residual-stress-induced normal load, L_{res}. Therefore, the residual stress in a welded joint can be evaluated by dividing L_{res} by the contact area, A_c, regardless of the stress state [12]:

$$\sigma_{res} = L_{res} / A_c \tag{7}$$

To evaluate the stress values from several indentation load steps, we performed multiple indentation and calculated the contact area directly from partial unloading curve at each analyzed load. In the instrumented indentation test, the contact area is determined by unloading curve analysis as shown in Fig. 1. By differentiation of the power-law fitted unloading curve at maximum indentation depth, we can get the contact depth as shown in Eq. (1). [6] And contact area, A_c calculated from the contact depth based on the geometry of the Vickers indenter.

$$A_c = 24.5 h_c^2 \tag{8}$$

Consequently, residual stress was calculated from the analyzed contact area in Eq. (8) and the measured load change, L_{res} by the effect of residual stress shown in Eq. (6).

3. RESULTS AND DISCUSSION

Sample Preparation

The samples used in this study are API X65 steel plates with the diameter 30 inch and 17.5mm thickness of Natural gas transmission pipeline and A335 P12 steel of cold reheater pipeline of fossil power plant facilities with a 17.9 mm thickness.

Table 1. Chemical composition of API X65 and A335 P12 used in this work as the base material (wt %).

Comp (wt%)	C	P	Mn	S	Si	Cr	Mo	Fe
API X65	0.08	0.019	1.45	0.003	0.31	-	-	Bal
A335 P12	0.08	0.01	0.45	0.01	0.31	1.15	0.55	Bal

Table 2. Welding Materials and conditions for girth welded joint

Materials	Welding Method	Filler Metal	Groove shape
API X65	GTAW+ SMAW	AWS ER70S-G AWS E9016-G	V
A335 P12	GTAW+ SMAW	AWS ER80S-G AWS E8016-G	X

The chemical compositions of the specimens are summarized in Table 1. Also the welding materials and welding conditions are summarized in Table 2. Mechanical testing samples were obtained from the joint

with the size of 10mm×50mm×17.5mm. The samples were ground with emery paper and finally polished with 1μm diamond paste.
In the case of the weld joint of A335 P91 steel, no significant defects were found in the completed weldments by the non-destructive X-ray examination. Additionally, post weld heat treatment (PWHT) were conducted on part of the samples for residual stress relaxation. The results taken from the PWHT specimens were compared with those from the as-welded specimens.

Tensile Properties of Three Microstructurally Characteristic Regions

Testing machine is Advanced Indentation System TM made by Frontics, Inc. The spherical indenter is a tungsten ball of 0.5mm radius. In the experiment for flow properties, the maximum indentation depth was 250μm, and 25 partial unloadings down to 70% of maximum load at each point were applied. All loading and unloading speed was 0.2mm/min. Advanced indentation test was done along the 3 lines of outer, middle and inner part of the weld joint thickness. And then, the microstructure of the tested sample was observed optically. The regions of weld metal, HAZ and base metal were distinguished using the optical metallography and conventional research of the variation of microhardness.

The boundary between heat-affected zone (HAZ) and base metal was identified 7mm apart from the fusion line using optical metallography and microhardness data for girth welded joint. The multiple indentation load-depth curves from three regions were superposed as shown in Fig. 8.

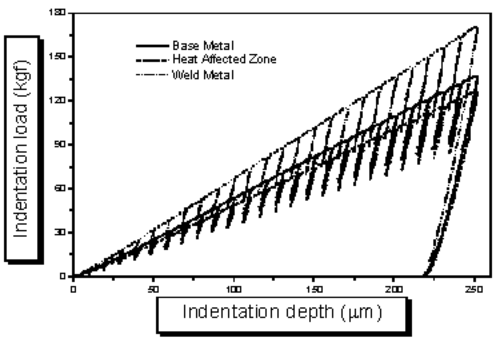

Fig. 8. Variation of indentation load-depth with the change of microstructures.

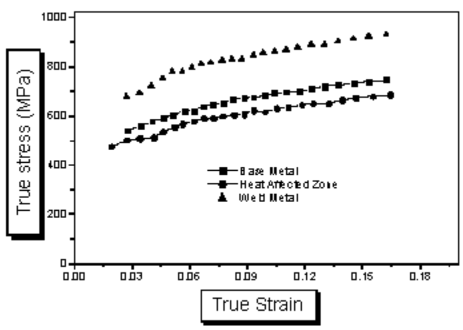

Fig. 9. The difference of flow properties with the change of microstructures.

Comparing the maximum indentation loads at the same indentation depth, it was found the material resistance to deformation was high as the sequence of weld metal, base metal and HAZ. The true stress-strain behaviors were obtained from each indentation curves. Generally, the higher yield strengths were evaluated for weld metal and base metal than that of HAZ as expected from indentation load-depth curve. Especially, the yield strength of HAZ was lower than base metal as shown in Fig. 9. It is due to the softening phenomenon during welding process [13], generally observed in HAZ of thermo-mechanical control processed (TMCP) steel such as the steel used in this study. And, HAZ can be identified as the weakest point for plastic deformation. The variation of yield strengths for outer, middle and inner lines was analyzed for the entire girth weld joint as shown in Fig. 10. The yield strengths of HAZ in the inner line were lower than those of HAZ in outer and middle lines. This phenomenon was explained by the annealing heat treatment of the constant heat input from outer welding paths.

Next, to assess the reliability of the advanced indentation test, the true stress-strain properties of base metal from advanced indentation test is compared with the result from the uniaxial tensile test. The uniaxial tensile testing was done using the thin plate specimens obtained from 3 parts of thickness direction. The gauge length, width and thickness of the sample were 25mm×6mm×4mm. The yield strengths of outer, middle and inner lines were 490, 440 and 495MPa, respectively. And, the ultimate tensile strengths of outer, middle and inner lines were 628, 535 and 625MPa, respectively. And, the flow properties from advanced indentation testing were summarized as below. The yield strengths of outer, middle and inner lines from advanced indentation were 453, 451 and 467MPa, respectively. And, the ultimate tensile strengths of outer, middle and inner lines were 718, 726 and 683MPa, respectively. Based upon the comparison of the test results, it is known that the advanced indentation test can be successfully used for nondestructive evaluation of tensile properties.

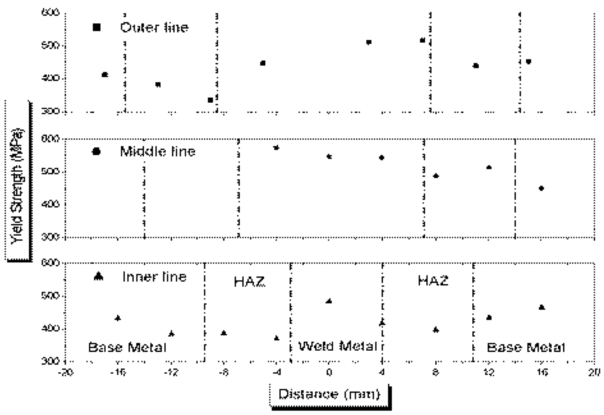

Fig. 10. Variation of the yield strengths for outer, middle and inner lines of the girth weld joint

<u>**Comparison of Residual Stresses between Saw-Cutting Technique and New Indentation Technique**</u>

In order to evaluate the residual stress of the weldment, two kinds of testing methods were performed at both PWHT and as-welded specimens; nondestructive indentation and destructive saw-cutting tests. Results from the indentation tests were compared with those from saw-cutting method for validation of the advanced indentation method.

To measure the distribution of the longitudinal residual stress by saw-cutting technique, strain gauges were attached along the distance from weld centerline. The relaxed strain values were easily converted to the residual stress by multiplying the elastic modulus. The indentation tests were performed before and after cutting. Indentation arrays using Vickers indenter was made on the polished surface near the cutting line at intervals of 5 mm. Maximum load and loading-unloading speed were 50 kgf and 0.5 mm/min, respectively. After cutting, indentation tests were also performed at the nearest location (3mm) from cut line, the results of which were used as reference or stress-free states. Residual stress is calculated by comparison of two indentation tests before and after cutting

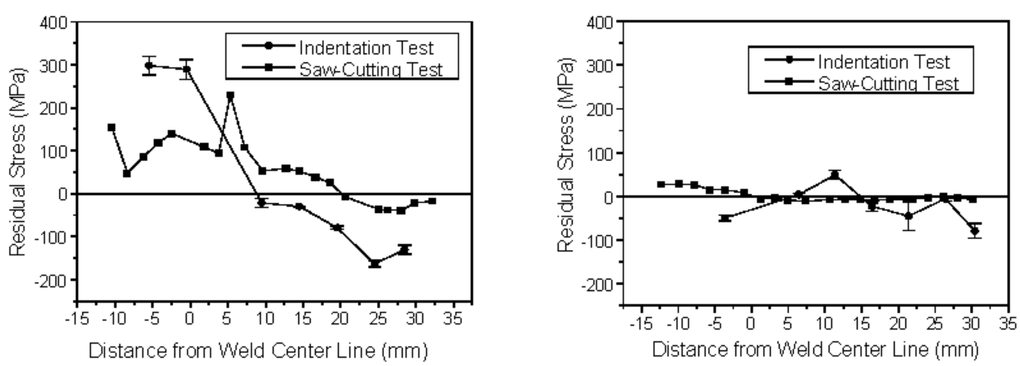

(a) **(b)**

Fig. 11. Direct comparison of residual stresses measured by indentation technique with those obtained from saw-cutting tests; (a) as-welded specimen (before PWHT) and (b) PWHT specimen.

Figure 11 summarizes the results from saw-cutting tests and indentation technique showing the distribution of longitudinal residual stresses of both PWHT and as-welded specimens. First saw-cutting tests shows the maximum residual stress existing near the weld centerline in as-welded specimen, i.e. specimen before PWHT, is up to 250 MPa, which is over the minimum required yield strength (220 MPa) of the A335 P12 steel used as base metal of the pipe. The high residual stress disappeared in PWHT specimen, as easily expected. So, it could be recognized that, post weld heat treatment is very effective in relaxing residual stresses. The variation in residual stresses measured by indentation tests also is similar to those in saw-cutting tests. High residual stresses observed in as-welded specimen were clearly relaxed.

Comparing residual stresses measured by indentation test with those by saw-cutting test, there was a little difference in stress values. The reason of difference is due to the difference in the kind of residual stresses measured in each test. In the case of stress measured by indentation technique is bi-axial stress including both longitudinal and transverse stress while residual stresses obtained from saw-cutting tests are just longitudinal stress. From all above results, it could be concluded that advanced indentation technique can be applied to non-destructive evaluation of welding residual stress of industrial facilities.

5. CONCLUSIONS

Advanced indentation technique was used to evaluate variation of the flow properties of API X 65 girth welded joint and residual stress of A335 P12 steels girth welded joint. The degree of deformation resistance was compared for weld metal, HAZ and base metal with indentation load-depth curve and evaluated yield strength. Weld metal was identified as the highest value among the three regions. And, HAZ had the lowest value. Therefore, HAZ was the weakest point for plastic deformation. By comparing with the results from conventional saw-cutting tests, it was found that the indentation tests could be used for quantitative/non-destructive assessment of welding residual stresses in industrial facilities or structures.

REFERENCES

[1] Kim, B.C., Lee, S., Kim, N.J., and Lee, D.Y.: Metallurgical Transactions A, 22A(1991), p.139
[2] Noyan, I. C. and Cohen, J. B., 1987, “Residual Stresses,” Springer-Verlag, New York.
[3] Ahn, J.-H., Choi, Y., and Kwon, D.: Journal of the Korean Institute of Metal and Materials, 38(2000), p. 1606.
[4] Ahn, J.-H. and Kwon, D.: J. Mater. Res., Vol. 16(2001), p. 3170.
[5] Francis, F.A.: Journal of Engineering Materials and Technology Transaction ASME, 98(1976), p. 272.
[6] Oliver, W.C., and Pharr, G.M.: Journal of Materials Research, 7(1992), p.1564.
[7] Norbury, A.L., and Samuel, T.: Journal of Iron and Steel Institute, 1179(1928), p. 673.
[8] Hill, R., F.R.S., Storåkers, B., and Zdunek, A.B.: Proceedings of Royal Society in London, A423(1989), p. 301.
[9] LaFontaine, W. R., Paszkiet, C. A., Korhonen, M. A. and Li, C.-Y.: J. Mater. Res., 6(1991), p. 2084.
[10] Tsui, T. Y., Oliver, W. C. and Pharr, G. M.: J. Mater. Res., 11(1996), p. 752.
[11] Suresh, S. and Giannakopoulos, A.E.: Acta mater., 46(1998), p. 5755.
[12] Lee, Y.-H. and Kwon, D.: J. Mater. Res. (in press).
[13] Youn, J.G. and Kim, H.J.: Journal of the Korean Welding Society, 6-2 (1988), p. 9-18.